

**ZIF-67-derived edge-oriented graphene clusters coupled with carbon nanotubes
containing encapsulated Co nanoparticles for high-frequency electrochemical
capacitors**

Wenyue Li^a, Nazifah Islam^b, Sakibul Azam^a, Zhen Xu^a, Juliusz Warzywoda^c, and
Zhaoyang Fan^{a*}

^a *Department of Electrical and Computer Engineering and Nano Tech Center, Texas
Tech University, Lubbock, Texas, 79409, USA*

^b *BaoNano, LLC, Lubbock, Texas 79415, USA*

^c *Materials Characterization Center, Whitacre College of Engineering, Texas Tech
University, Lubbock, Texas 79409, USA*

* *Email: zhaoyang.fan@ttu.edu*

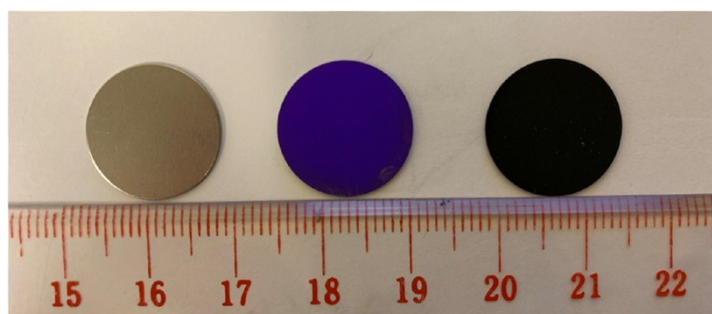


Figure S1. Digital photos of (left to right) SS disk, SS disk covered with ZIF-67 and SS disk covered with C-ZIF.

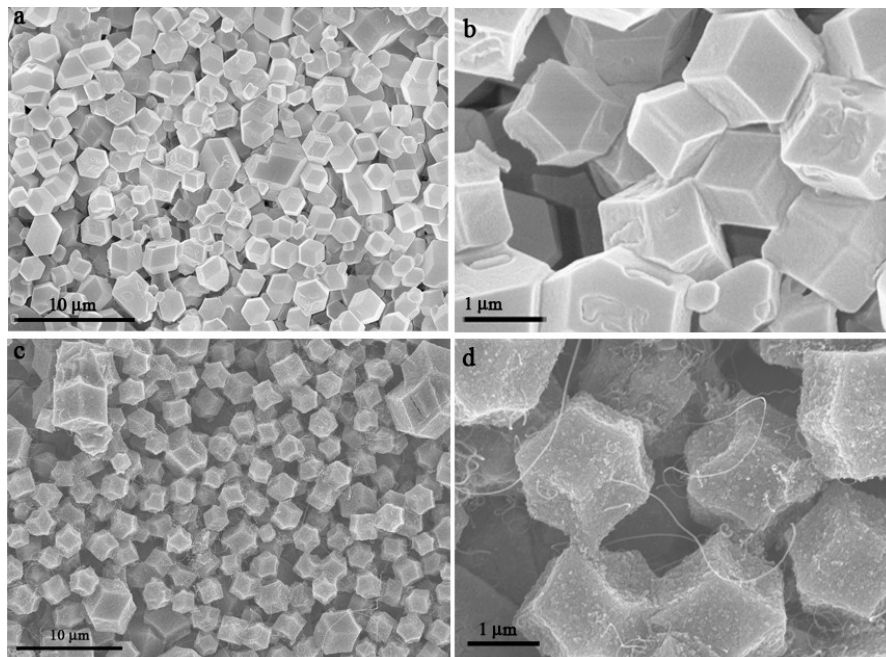


Figure S2. SEM images of ZIF-67 (a, b) and C-ZIF (c, d) particles. Thermal carbonization of ZIF-67 was conducted by plasma heating but the sample was shielded from the incident plasma species by graphite shielding. Sparse CNTs were formed from the adventitious plasma carbon species, and CNTs growth was catalyzed by Co NPs.

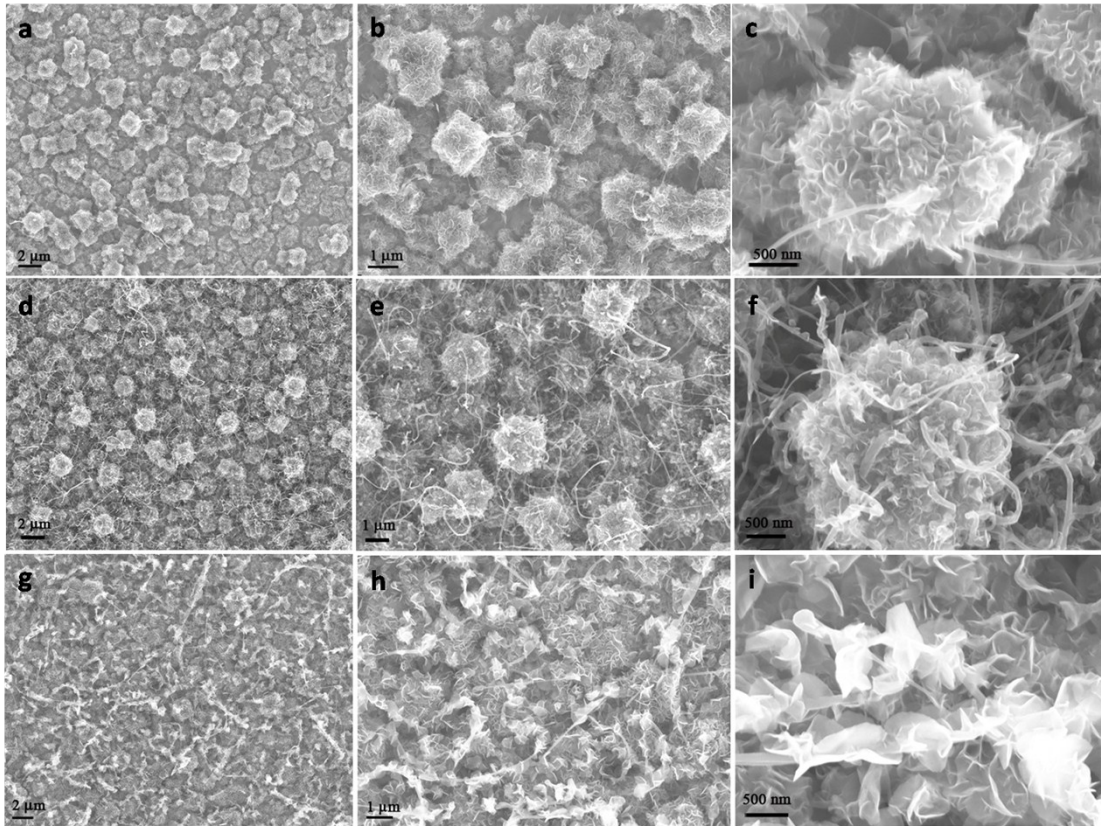


Figure S3. SEM images showing a comparison of the morphological changes for samples C-ZIF/SS-3 (a-c), C-ZIF/SS-5 (d-f) and C-ZIF/SS-8 (g-i), which were caused by a different plasma treatment duration.

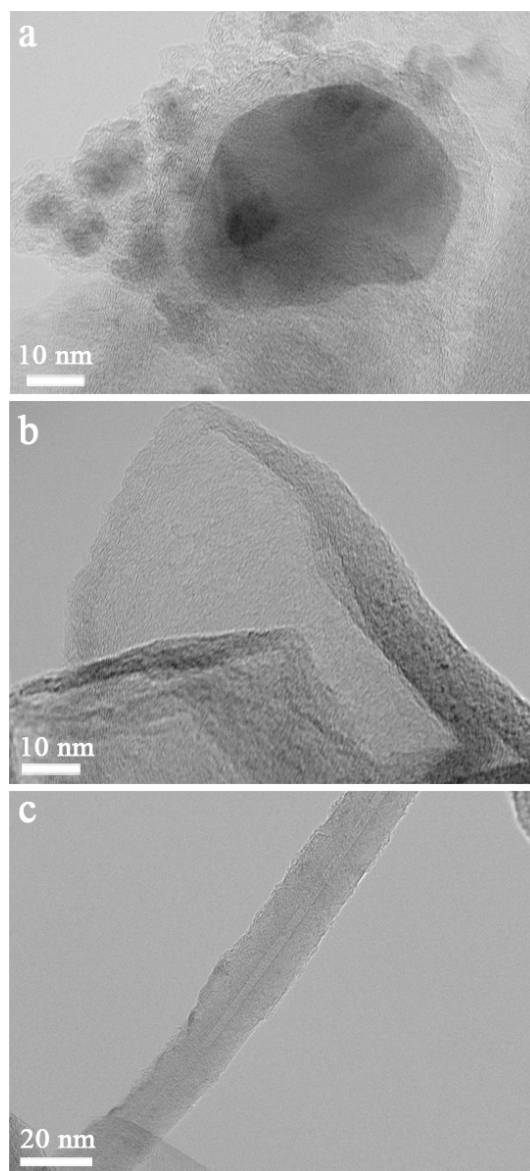


Figure S4. HRTEM images of Co NP encapsulated in graphitic carbon shell (a), EOG (b) and CNT (c).

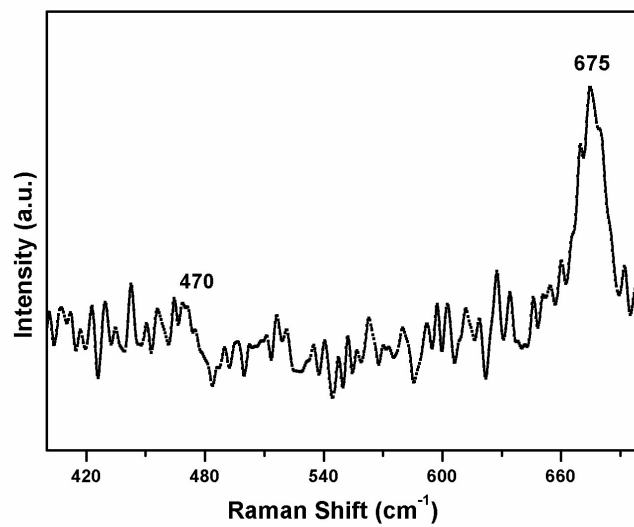


Figure S5. Enlarged part of the Raman spectrum for sample C-ZIF/SS.

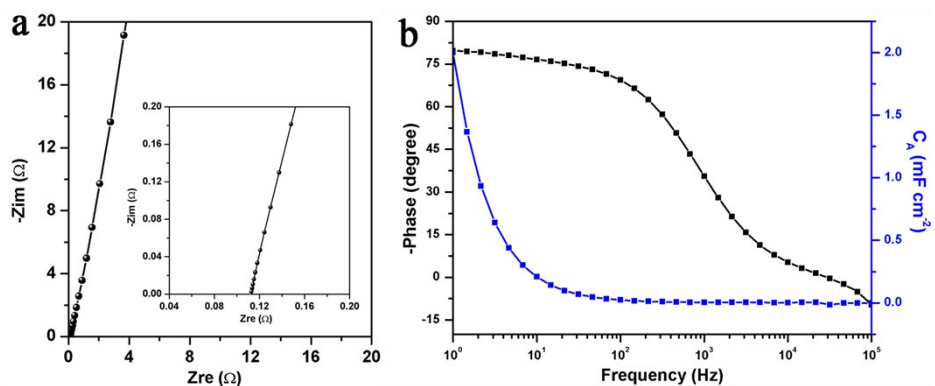


Figure S6. Nyquist spectrum (inset shows the high-frequency region) (a) and Bode diagram and areal capacitance vs. frequency plot (b) for the C-ZIF/SS-based cell in 6 M aqueous KOH electrolyte.

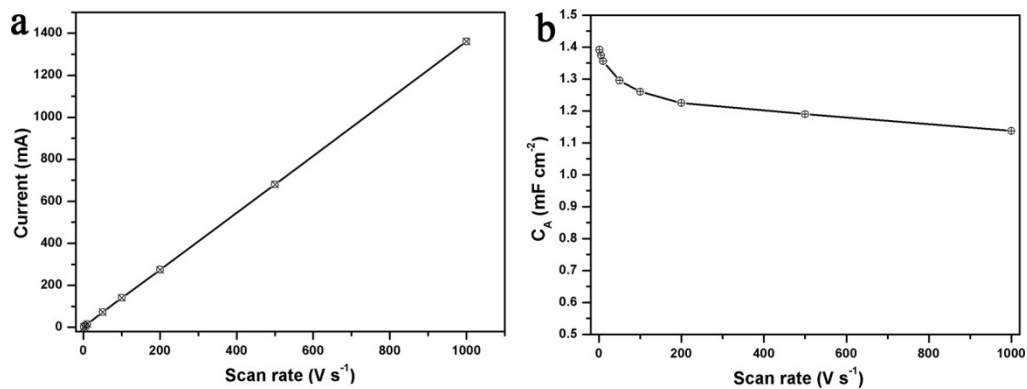


Figure S7. Plot of current density vs. scan rate (a) and areal capacitance vs. scan rate (b) for the C-ZIF/SS-5-based cell.

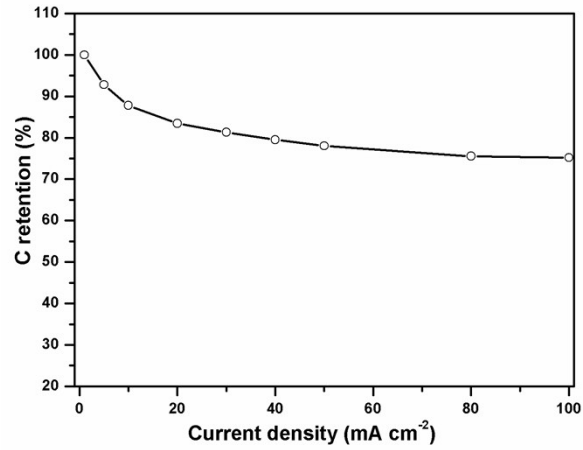


Figure S8. Capacitance retention under different current densities in GCD measurements for the C-ZIF/SS-5-based cell.

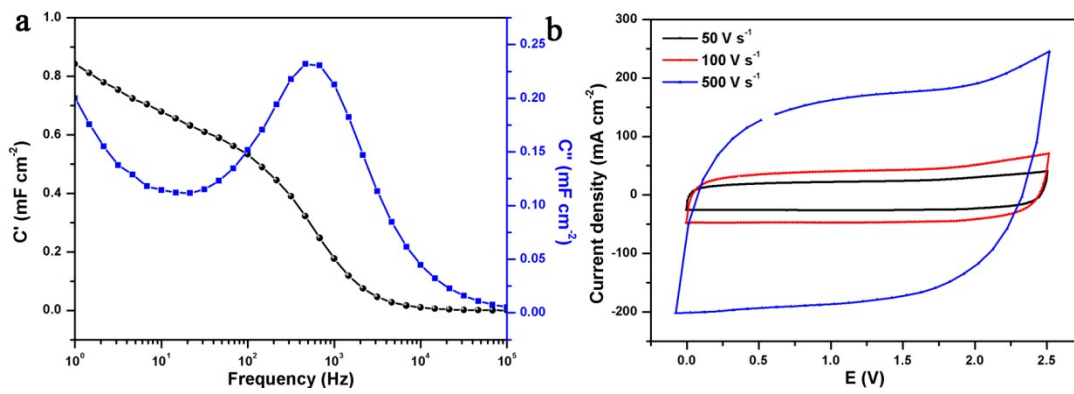


Figure S9. Real and imaginary components of the complex capacitance and their dependence on frequency (a), and CV curves for different scan rates (b) for the C-ZIF/SS-8-based cell.

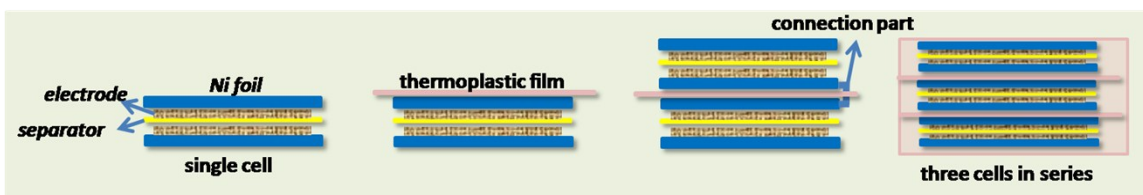


Figure S10 Schematic process of preparing three cells in series sealed in thermoplastic films.

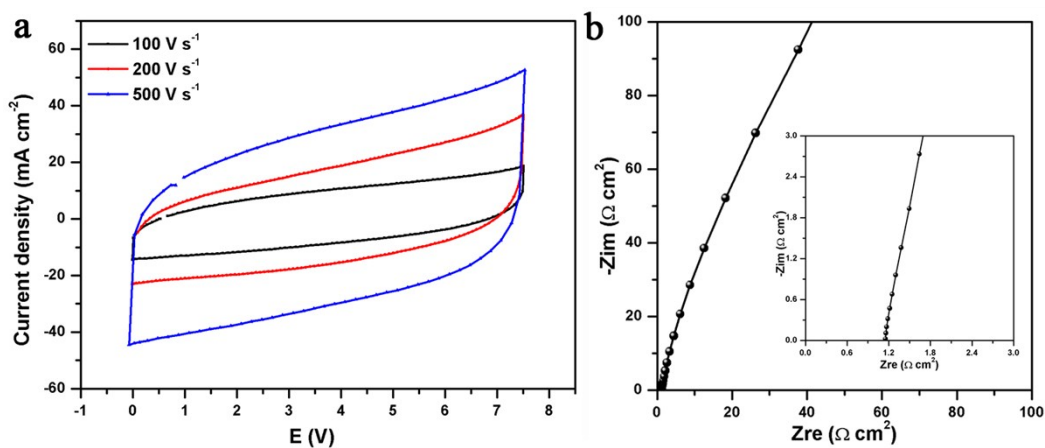


Figure S11. CV curves (a) and Nyquist plot (b) of the 7.5 V cell.